Contact UKCEH NORA team at
noraceh@ceh.ac.uk

What's on the outside matters – surface charge and dissolve organic matter association affect toxicity and physiological mode of action of polystyrene nanoplastics to *C. elegans*

Carolin L. Schultz[1], Sylvain Bart[1,2], Elma Lahive[1], David J. Spurgeon[1,*]

[1] UK Centre for Ecology and Hydrology, Wallingford, OX10 8BB, United Kingdom

[2] Department of Environment and Geography, University of York, Heslington, York, YO10 5NG, UK

* Corresponding author: David J. Spurgeon, email: dasp@ceh.ac.uk

22   ABSTRACT

23   To better understand nanoplastic effects, the potential for surface functionalisation and

24   dissolve organic matter eco-corona formation to modify the mechanisms of action and toxicity

25   of different nanoplastics needs to be established. Here we assess how different surface

26   charge modifying functionalisation (postive (+ve) aminated; neutral unfunctionalised; negative

27   (-ve) carboxylated) altered the toxicity of 50-nm and 60-nm polystyrene nanoplastics to the

28   nematode *Caenorhabditis elegans*. Potency for effects on survival, growth and reproduction

29   reduced in the order +ve aminated > neutral unfunctionalised >> –ve carboxylated with toxicity

30   >60 fold higher for the +ve than -ve charged forms. Toxicokinetic-toxicodynamic modelling

31   (DEBtox) showed that the charge related potency was primarily linked to differences in effect

32   thresholds and dose associated damage parameters, rather than to toxicokinetics parameters.

33   This suggests that surface functionalisation may change the nature of nanoplastic interactions

34   with membrane and organelles leading to variations in toxicity. Eco-corona formation reduced

35   the toxicity of all nanoplastics indicating that organic molecule associations may passivate

36   surfaces. Between particles, eco-corona interactions resulting in more equivalent effects,

37   however, even despite these changes, the order of potency of the charged forms was retained.

38   These results have important implications for the development of future grouping approaches.

39

40   **Keywords:** Nanoplastic, Surface charge, Physiological mode of action, Toxicodynamics, Eco-

41   corona

42

43   TOC art

44
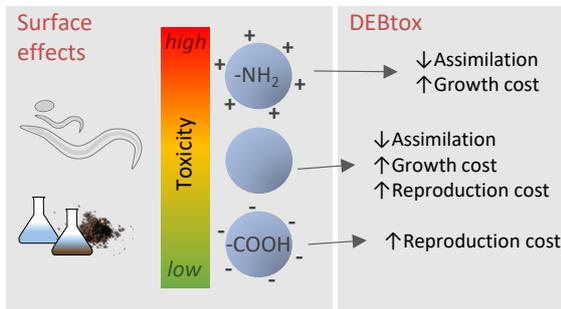
46

47

48

49   INTRODUCTION

50   The environmental fate and toxicity of polymeric nanomaterials (particle with dimension <100

51   nm, also termed "nanoplastics") is of increasing interest given their emerging use in products

52   and processes (see [1]). Added to this primary nanoplastics load is a theorised as increasing,

53   but as yet poorly characterised, environmental burden arising from fragmentation of larger

54   plastics[2,3]. With increasing recognition of the potential load of nanoplastics reaching the

55   environment, there is a need to understand the drivers of any toxicity resulting from exposures

56   to these materials[4,5].

57

58   Previous work has shown that nanoplastics can be accumulated in the intestine[6] and other

59   tissues of exposed organisms[7,8]. Nanoplastic exposure has been shown to affect survival,

60   growth and reproduction (e.g. [6,9]), with effects linked to mechanisms associated with oxidative

61   stress, such as genotoxicity, cell membrane damage, mitochondrial damage, different

62   epigenetic effects (e.g. microRNA expression) and changes in insulin signalling and energy

63   metabolism[10-14]. A critical finding in nanotoxicology has been the role that surface properties

64   can play in determining effects[15-18]. For example in *C. elegans*, bioaccumulation and mortality

65   following exposure to positive (+ve) CeO_2 nanoparticles was greater than for neutral or

66   negative (-ve) forms[19]. Similarly, Bozich et al.[20] found +ve gold nanoparticles toxicity was an

67 order of magnitude greater than for –ve forms in *Daphnia magna*. Higher toxicity of +ve, than

68 neutral or -ve nanoparticles, is further supported by studies in bacteria[16] and zooplankton[21].

69

70 Greater toxicity of +ve (e.g. aminated) nanoparticles has been linked to their potential for

71 stronger interactions with -ve cell surfaces[22]. Evidence has been found that surface charge

72 can change nanoplastic toxicokinetics (TK) resulting in differences in tissue localisation[23,24].

73 However, whether these effects are alone enough drive variations in toxicity, or whether

74 surface charge may also alter mechanisms of action leading to differences in toxicodynamics

75 (TD), is currently not known. In species where full life-cycle testing is possible, such as the

76 nematode *C. elegans*, analysis of time series effects on life-cycle traits can be used to

77 parameterised dynamic energy budget theory based TK/TD (DEBtox) models [25,26]. These

78 TK/TD approaches can be used to determine whether differently charged nanoplastics exert

79 toxicity through the same or different of four physiological modes of action (pMoAs) namely: i)

80 assimilation, ii) increase in maintenance, ii) growth or iv) reproduction costs[27].

81

82 As for other nanomaterials, nanoplastics can be transformed through the association of

83 dissolved organic molecules with the particle surface to form an "eco-corona". Eco-corona

84 formation has been found to alter the bioavailability and toxicity of nanomaterials[21,28]. Further,

85 because the eco-corona can overcoat, or even partially or completely replace, the engineered

86 coating[29], the presence of adsorbed organic molecules has the potential to reduce the

87 variation between charged forms in their environmental behaviour, bioavailability and

88 toxicity[17], including for nanoplastics[30]. However, the extent to which eco-corona formation may

89 modify the mode of action, and resulting toxicity of nanoplastics is not established.

90

91 To evaluate the potency and identify the pMoA and TK/TD parameters of differently charged

92 polystyrene nanoplastics, we here conducted partial and full life-cycle toxicity tests with *C.*

93 *elegans*. DEBtox modelling was used to identify the pMoA and associated TK/TD traits for the

94 life-cycle data. Our hypothesis was that nanoplastic surface charge would influence the TK

4

95 rates, but not PMoA or the TD parameters. This assumption being because the surface charge

96 may affect cell surface interactions, but not the intracellular fate after internalisation. To further

97 assess the relevance of nanoplastic surface charge for toxicity under more realistic

98 environmental media exposure conditions, we next investigated how the presence of

99 dissolved organic matter species altered the toxicity of the differently charged particles in a

100 soil pore water extract. Our hypothesis was the formation of a surface eco-corona composed

101 from the dissolved organic molecules present would reduce dissimilarities in the toxicity of

102 differently charged nanoplastics in this more realistic exposure setting.

103

104

105 MATERIALS AND METHODS

106 Nanoplastics

107 Six spherical polystyrene nanoplastics were tested for toxicity to the nematode *C. elegans*.

108 These were three 50-nm yellow-green fluorescently labelled particle that were immediately

109 available and later three 60-nm unlabelled nanoplastics (all Magsphere, Pasadena, USA)

110 (Table 1). These particles have been used in previous nanotoxicology studies, which have

111 demonstrated their chemical properties and charge[31,32], with the positive and negative charge

112 status supported by our zeta potential measurements (Table 1). An initial set of experiments

113 was conducted with the 50-nm set. This set was immediately available for experimental use

114 for our study, but carried a fluorescent label. During the time these experiments were being

115 conducted, a second set of differently charged nanopolystyrene particles became available

116 through the same supplier. A second set of tests using this 60-nm set were, therefore,

117 conducted to confirm the observations made relating to charge effects to cross-validate the

118 responses seen. For each particle size set, one unfunctionalised ("50PSF^0" and "60PS^0"), one

119 aminated ("50AMF$^+$" and "60AM$^+$") and one carboxylated ("50CAF$^-$" and "60CA$^-$") giving,

120 respectively, neutral, +ve and -ve surface charges were tested for toxicity. The particles, thus,

121 represent two independent sets of differently charged nanoplastics of different size, but with

122 the same set of surface functionalisation. Transmission electron microscopy (TEM) size data

123   was provided by the supplier (Table 1). To confirm size and charge status, the hydrodynamic

124   diameter and zeta potential of each nanoplastic were measured using dynamic light scattering

125   (DLS) (Zetasizer Nano ZS, Malvern Panalytical) in exposure media without the *E. coli* bacteria

126   present which can compromise assessment in *C. elegans* test systems.

127

128   Table 1: Nanoplastic physicochemical properties: mean manufacturer stated transmission

129   electron microscopy diameter ± SD (nm), for manufacturer certificate of assurance.

130   Measured DLS hydrodynamic diameter ± SD (nm) and zeta potential ± SD, n=3.

	TEM size (nm) ± SD	DLS Z-Average (nm) ± SD	Zeta potential ± SD
50PSF^0	50 ± 12	51.8 ± 0.3	-22.3 ± 29.4
50AMF$^+$	50 ± 10	51.0 ± 0.4	+38.6 ± 18.4
50CAF$^-$	49 ± 7	50.8 ± 0.3	-59.4 ± 17.8
60PS^0	64 ± 18	69.3 ± 0.8	-37.0 ± 14.0
60AM$^+$	61 ± 9	59.8 ± 0.6	+51.8 ± 17.0
60CA$^+$	63 ± 20	64.9 ± 0.7	-49.0 ± 11.1

131

132

133   Exposure media and nematode toxicity assays

134   All experiments were carried out with *C. elegans* wild-type strain N2 initial obtained from the

135   *C. elegans* Genetics Centre (Minneapolis, USA). All nematodes used were reared from this

136   ancestral line in cultures maintained at 20˚C on nematode growth medium plates and *ad*

137   *libitum* fed the uracil-deficient *Escherichia coli* strain OP50 (*C. elegans* Genetics Centre)[33].

138

139   Partial and full life-cycle exposures in SSPW and LUFA2.2 pore water

140   Partial life-cycle toxicity tests were conducted with the 50-nm nanoplastic set in a simulated

141   soil pore water (SSPW) media (composition following the recipe of Tyne et al.[34] prepared

142   without Fe and fulvic acid (and so in the absence of intentionally added dissolved organic

ligands). The SSPW was supplemented with 2 mg/L cholesterol (Sigma Chemicals) to ensure

normal nematode growth, development and reproduction and *Escherichia coli* strain OP50 (at

a standard density of O.D. 0.12/day consistent with previous studies[35]) added as a food

source. For all tests, nematode eggs were initially obtained by bleaching[36]. These age

synchronised eggs were immediately exposed to the nanoplastics in a series of concentrations

range of 0, 1, 2.8, 7.1, 18.8 and 50 mg/L in a fully randomised design in 12 well plates (Greiner

Bio One, Stonehouse, UK), with 1 mL SSPW and 5 replicates for each tested concentration

at 20°C for exposures in constant dark. Initially approximately 50 eggs were transferred into

each well and after 72 h two randomly selected adults were transferred to fresh medium for a

further 72 h to track growth and lay eggs (total exposure time 144 h). The two individuals

transferred after 72 h were photographed using a VC.3036 HD-Ultra Microscope Camera

(PeplerOptics, Knutsford, UK) mounted on a Nikon SMZ 800 microscope (Nikon Corporation,

Tokyo, Japan). The volumetric length (cubic root of body volume) of each individual was

calculated using a cylinder with rounded ends as approximation of the nematode shape,

$volumetric\ length = \sqrt{(\pi * A^2)/(8*l)}$, where l = length [μm], A = area [μm^2]. Produced juveniles

and eggs were stained at the end of the experiment with a 1% Rose Bengal solution (Sigma

Chemicals, Pool, UK) for 40 min and subsequently killed by heating to 55°C for 1 h for

counting.

To exclude the possibility that any observed nanoplastic toxicity was caused by the presence

of surfactants, synthesis residues or other contamination in the supplied stock dispersions,

additional exposures were carried out with the dispersion medium alone after the particles

were removed. These additional assays were conducted at a concentrations of dispersion

medium to that equivalent which caused no effect and full reproduction knock-down for each

nanoplastic in partial and full life-cycle tests for each of the 50-nm and 60-nm nanopolystyrene

sets respectively. Samples of the supernatant free of particles were prepared by Amicon Ultra-

4 10 kDa ultrafiltration (Millipore) of the nanoplastic dispersion. Experiments were conducted

following the same protocol as used for the partial life-cycle exposures described above.

171

172   To investigate the pMoA and associated TK/TD parameters for the differently charged

173   nanoplastics, life-cycle toxicity tests were carried out also in the SSPW medium. For the 50-

174   nm nanoplastic set, age synchronised eggs were first obtained by bleaching and immediately

175   exposed to different concentrations (2-200 mg/L) of each charge variant nanoplastic. All

176   exposures were carried out in a fully randomised design in 12 well plates (Greiner Bio One)

177   with 1 ml exposure medium per well, two individuals per well and 5 replicates for each of a

178   series of tested concentrations ranging from 1-50 mg/L for the 50 nm –ve and neutral particles

179   and from 1-200 mg/L for the remaining particles. These concentration ranges were selected

180   to ensure a sufficient number of sublethal treatments to provide data for effect modelling in all

181   cases. The nematodes were transferred into fresh medium at 3 day intervals during the

182   juvenile growth phase and then daily during the egg laying period (Day 3 to Day 8) in order to

183   allow reproduction to be assessed daily as needed as input data for DEBtox modelling.

184   Survival was checked daily and growth assessed by photographing individuals in the exposure

185   wells daily up to 10 days after the start of the exposure using a VC.3036 HD-Ultra Microscope

186   Camera (PeplerOptics, Knutsford, UK) mounted on a Nikon SMZ 800 microscope. To measure

187   reproduction, after adults were removed each day, the juveniles and eggs were stained and

188   killed as described above. Brood-size for each individual was given as the sum of offspring

189   produced over all days. To confirm our observation of surface change effects on responses

190   over time, a second set of full life-cycle tests were conducted with the larger 60-nm nanoplastic

191   set. The tests were conducted in the SSPW medium, but in this case randomised in 6 well

192   plates with 2 mL medium and 1 adults per well. Analysis for these two independent

193   experiments was used to verify identified charge effects on life-cycle traits and pMoA and

194   TK/TD parameters through DEBtox modelling.

195

196   To assess eco-corona formation effects on differently charged nanopolystyrene toxicity, an

197   additional set of partial life-cycle toxicity tests was conducted under more realistic conditions

198   in an extracted soil pore water containing natural dissolved carbon species that could attach

199   to the particle surfaces. The soil used for pore water preparation was the well characterised

200   standard soil LUFA2.2 (LUFA Speyer, Germany), a loamy sand with an organic carbon content

201   of 1.7%, a pH_{CaCl2} of 5.6 and a water holding capacity (WHC) of 42 mL/100 g. To collect the

202   pore water extract, the soil was wetted to 50% water holding capacity with deionised water for

203   24 h after which the water content then increased to 100% WHC for an additional 24 h. Pore

204   water from the saturated soil was extracted by 0.2 µm vacuum filtration using a surfactant free

205   Rapid Flow cellulose membrane filter (Nalgene Inc, Rochester, USA). Both SSPW and

206   LUFA2.2 pore water were supplemented with 2 mg/L cholesterol (Sigma Chemicals) and food

207   source *Escherichia coli* strain OP50 (at O.D. 0.12/day). The toxicity of the different surface

208   charge nanoplastics in the extracted LUFA2.2 pore water was assessed for both the 50-nm

209   fluorescent nanoplastic ($50PSF^0$, $50AMF^+$, $50CAF^-$) and 60-nm nanoplastic ($60PS^0$, $60AM^+$,

210   $60CA^-$) sets. Studies were conducted using the same partial life-cycle test method detailed

211   above for the 50-nm particle SSPW experiments.

212

213   Toxicity data analysis and DEBtox modelling

214   The partial life-cycle toxicity test data was analysed for concentration-response relationships

215   in Systat Sigmaplot 13.0 using a 3-parameter logistic regression to estimate median effect

216   concentration (EC_{50}), upper asymptote, and slope parameters for each nanoplastic and test

217   media combination. Concentration–response curves for the differently charged nanoplastics

218   were compared using the F test[37] to investigate differences in fitted relationships for each

219   functionalised nanoplastic pair, a $p<0.05$ indicating a significant difference in response

220   between the two differently charged forms.

221

222   DEBtox modelling was conducted using the latest variant model of Jager[38] based on the

223   DEBkiss model, which is a well-established approach for the analysis of life-cycle toxicity test

224   data. The model follows a TK/TD formulation explicitly taking damage into consideration as in

225   the General Unified Threshold model for Survival (GUTS)[39]. This formulation of DEBtox is

226   available as a package of the Build Your Own Model (BYOM) modelling platform coded in

9

227   Matlab (debtox.info/byom.html). As suggested by Jager[38], we first fitted the control treatment,

228   and once calibrated kept the non-toxicological parameters fixed to fit the toxicological

229   parameters for the different nanoplastic effect data-sets. The growth of *C. elegans* is often

230   described with initial food limitation[26,40], however, as growth monitoring started one day after

231   hatching this early stage food limitation could not be assessed. Therefore, we assumed Van

232   Bertalanffy growth started one day after hatching as in Cedergreen et al.[41], which indeed well

233   described growth in the control condition. The reproductive behaviour of *C. elegans* stops

234   rather abruptly when the stored sperm cells runs out (sperm production stops when egg

235   production commences, which usually happened when approximately 300 offspring have

236   been produced). Therefore, we only used reproduction data up to t = 6 days to avoid this

237   complexity arising due to sperm limitation. The DEBtox model was used to identify the best

238   fitting primary pMoA or combination for each functionalised nanoplastic from four possibilities:

239   i) assimilation, ii) increase in maintenance, ii) growth or iv) reproduction costs. We tried the

240   different pMoA combinations and selected the best fit based on the relative goodness-of fit

241   with the minimal log-likelihood.

242

243

244   RESULTS AND DISCUSSION

245   Tests for effects of dispersion medium on nematode reproduction

246   Previous studies have shown that apparent toxic effects initially assigned to micro- and

247   nanoplastics can instead be attributed to the presence of additives (e.g. the antimicrobial

248   sodium azide) and toxic synthesis residues in carrier solutions[42]. To exclude this possibility,

249   we specifically procured sodium azide free nanoplastics and conducted exposure to

250   nanoplastic free supernatants (Figure 1). These supernatant exposures did not show any clear

251   knock-down for reproduction (maximum difference from the control for any of the tested

252   supernatants for the 50-nm set, 21.2 juveniles, Hedge corrected effect size = 0.54; and 60-nm

253   set, 0 vs 2 mg/L 60AM, 40 juveniles, Hedges' G effect size 0.797). Overall the results indicate

254   that any strong knock-down effects of the tested nanoplastics can be attributed primarily to

255   the presence of the nanoplastics themselves in all cases and not to other chemicals present

256   in the supplied stock dispersions.

257

258
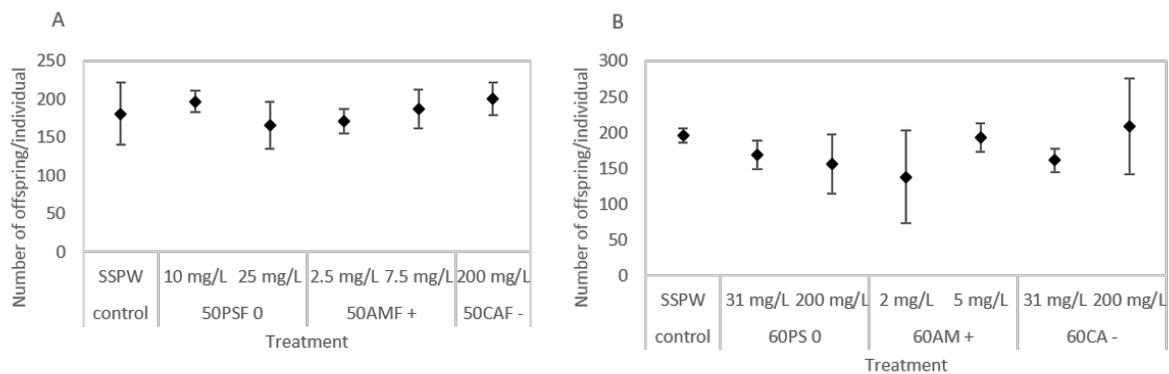
260   **Figure 1.** Test for the effect of the different dispersion media after removal of nanoplastic

261   particles from medium; these where dosed at concentrations, estimated from the main toxicity

262   test, which if containing the associated nanoplastic would have caused no effect or full knock-

263   down of nematode reproduction A) supernatants from the 50-nm fluorescent nanoplastics, B)

264   supernatants from the 60-nm unlabelled nanoplastics; values are means with standard

265   deviation based on 5 replicates.

266

267

268   Toxicity tests comparing charged nanopolystyrene toxicity in SSPW

269   An initial set of short-term toxicity tests were conducted for the differently charge nanoplastics

270   in the fulvic acid free SSPW. These tests indicated significantly higher toxicity for both

271   reproduction and growth (expressed as body length) for the +ve than the neutral or -ve forms

272   (F-test for comparison of concentration response relationships, $p<0.001$ in all cases) (Figure

273   2, Table S1). The neutral nanoplastics also showed higher toxicity than the -ve particles, which

274   showed minimal toxicity even at the highest tested concentration of 200 mg/L. Of the two

275   endpoints, reproduction was more sensitive than growth. For reproduction, the EC_{50} for the

276   50AMF$^+$ nanoplastics of 2.6 mg/L was 6 fold lower than that for the neutral particles (EC_{50} 18.1

277 m/L) and >75 fold lower than for the 50CAF⁻ nanoplastics (Figure 2A). For effects on growth,

278 while EC_{50} were higher than for reproduction, the order of potency was retained with the

279 50AMF⁺ (15.2 ± 1.3 mg/L) > 50PSF⁰ (40 ± 2.1 mg/L) >> 50CAF⁻ (>200 mg/L) (Figure 2B). The

280 higher toxicity of the +ve nanoplastics was confirmed using the reproductive broodsize data

281 from the full life-cycles experiments conducted in SSPW for the 60-nm particle (see Table S1

282 for full set of endpoint effects concentrations). These reproductive EC_{50} ± SE values indicated

283 potency ordered as 60AM⁺ (3.2 ± 0.3 mg/L) > 60PS⁰ (53.5 ± 5.2 mg/L) >> 60CA⁻ (>200 mg/L).

284 The maximum fold difference in toxicity for the +ve and neutral nanoplastics was >62.5 fold.

285
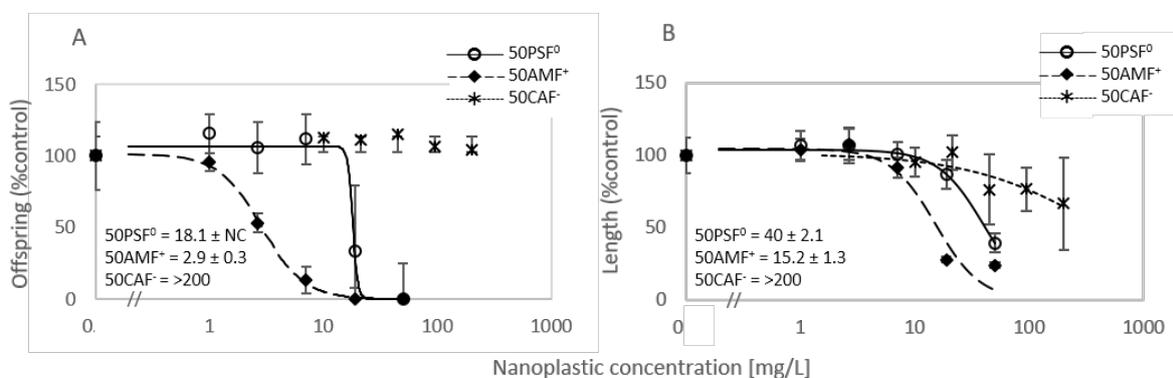
287 **Figure 2:** A. Offspring per individual after 6 days and B. volumetric length at 72 h as % of

288 control after exposure to 50PSF⁰ (open circle, solid line), 50AMF⁺ (closed diamond, dashed

289 line) and 50CAF⁻ (asterisks, dotted line) in SSPW, point are averages ± SD from n=5

290 replicates, line is 3-parameter log logistic regression fitted; stated values are EC_{50} (±SE) in

291 mg/L, NC = confidence intervals not calculable.

292

293 The higher toxicity of the +ve 50AMF⁺ and 60AM⁺ than their size matched neutral 50PSF⁰ and

294 60PS⁰ nanoplastics supports observations from previous studies with different charged

295 nanomaterials that have indicated a greater effect from particles with a positive surface charge

296 e.g.[21,43,44,45]. Although additionally studies have also shown greater effects of negatively

297 charged than neutral nanoparticles [46]. Reviewing the role of charge in cell surfaces and other

298 biological interactions, Forest and Pourchez[18] concluded there was evidence of preferential

299   binding of +ve nanoparticles due to electrostatic interactions with the predominantly -ve cell

300   membrane surface. This potential increase in nanoplastic-biomembrane interaction strength

301   points to a difference in TK mechanisms leading to higher uptake as a major driver of the

302   increased +ve nanoplastic potency. However, Forest and Pourchez[18] suggested that

303   attributing this higher +ve particle toxicity to surface interactions alone may be too simplistic.

304   In particular, the formation of a surface protein corona may modify both surface charge and

305   other surface properties, such as the ability of particle surface to be recognised by cells or the

306   nature of steric interaction, so affecting the nature of cell surface contacts and, hence, the

307   nature and strength of nano-bio interactions.

308

309   Using the same nanoplastics as tested here, Loos et al[43] also found higher toxicity for the

310   aminated than carboxylated forms. In this study, the higher +ve nanoplastic toxicity was

311   attributed not only to higher cell surface interactions, but also to the formation of holes in

312   biological membranes and to associated lysosomal swelling and rupture through continuous

313   activation of the lysosomal proton pump. An interaction of aminated nanoplastics with

314   lysosomes have also been found in *in vivo* in sea urchin embryo exposures[47] that may further

315   be linked to the increased activity of stress signalling pathways[48]. The charge related organelle

316   effects indicate that, as well as potentially modifying TK through changing cell surface

317   interactions to alter cellular uptake, charge status may also affect TD effects by inducing

318   different cellular damage pathways.

319

320   A higher toxicity of positively charged nanomaterials was also found by Hanna et al.[35].

321   However, these authors attributed this greater toxicity to the positively charged particles

322   agglomerating the *E. coli* bacterial food source, leading to reduced feeding and resulting

323   effects on growth and reproduction, rather than through a direct "toxic" effect. In our test

324   system, we cannot exclude that such a bacterial food interaction may play some part in the

325   greater effects observed for the positively charged particles. However, there are a few key

326   differences between our study and that of Hanna et al [35] that may limit the contribution of this

327 agglomeration interaction to observed effects. First, the two study were conducted in different

328 test media. Thus, Hanna et al.[35] conducted their test in relatively high ionic strength M9 buffer,

329 a test solution in which nanomaterials themselves have been found to readily agglomerate. In

330 contrast, in our study, SSPW was used as test media. This solution has been specifically

331 designed to better reflect soil pore water conditions and has a lower reduce ionic strength than

332 M9-buffer, leading to reduced agglomeration potential for nanomaterials and potentially

333 heteroaggregates of and with bacteria[49]. Secondly, the means by which particle surface was

334 charged differ significantly between the two studies. In Hanna et al.[35] the key finding of a

335 positive charge effect on *E. coli* aggregation to affect feeding related to observations for Au

336 nanoparticles. These materials were differently charged as a result of the addition of different

337 surface coatings. For the nanopolystyrenes tested here, charge was conveyed by different

338 functionalisation of the polymer surface groups. Coatings as used by Hanna et al.[35] can

339 dissociate from particle surfaces where they may directly interact with the bacteria present,

340 including by acting as a food source. The strongly attached surface functional groups on our

341 polystyrene particles on the other hand has no such known direct interactions with bacteria.

342 To confirm the extent of agglomeration caused for bacteria by the addition of the different

343 charged nanopolystyrenes in our test system, we looked for the presence of bacterial

344 aggregates in the exposure media at the exposure concentrations closest to reproductive EC_{50}

345 for each particle (Fig. S3). In exposure wells, limited presence of bacterial aggregates was

346 found in the 60AM, but were not observed in other treatment. Hence, based on these

347 differences and observations including limited observed bacterial aggregations, we concluded

348 that a charge effect on bacteria reducing feeding may not be the primary driver of the observed

349 different in responses to nanopolystyrene exposures. To further explore the observed effects

350 responses and associated energetic causes, we, therefore, proceeded to life-cycle testing and

351 DEBtox analysis.

352

353 Life-cycle exposures and DEBtox modelling for pMOA and TK/TD parameter identification

354   Full life-cycle tests data for the 50-nm and 60-nm charged particle sets in SPPW was used as

355   input to DEBtox models to calculate TK/TD traits. The full life-cycle toxicity tests supported

356   observations in short-term bioassays for the 50-nm nanoplastics in SSPW that potency of the

357   charge variants increased in the order +ve > neutral >> -ve (Figure S1, S2). The order of

358   toxicity and the magnitude of differences for each endpoint were consistent between 50-nm

359   and 60-nm sized sets (Figure 3 A-F, S1, S2). The charge effect on toxicity can be seen most

360   clearly for effects on reproduction, which was the most sensitive parameter consistent with

361   other life-cycle toxicity studies in *C. elegans*[26,50,51]. Thus, the -ve particle had no effect on

362   reproduction up to the highest tested concentration; the neutral particle had effects on

363   reproduction at treatments of 18.8 mg/L and higher and the +ve particles at 2.7 mg/L and

364   above. Effects seen on survival and growth all supported the greater toxicity of the +ve

365   compared to the neutral particles (Figure 3 A-F), the only exception being the slightly greater

366   effects of the $50PSF^0$ than $50AMF^+$ particles on survival, the reason for this difference being

367   currently unclear (Figure 3 A,B). The concentration dependent effects on all traits were largely

368   conserved between the similarly charged 50-nm and 60-nm nanoplastics. The similarity of the

369   observed effects confirm the repeatability of the charge effect, even in nanoplastics that differ

370   in size, albeit only by a relatively small extent.

A) 50 nm fluorescent polystyrene unfunctionalised (neutral)
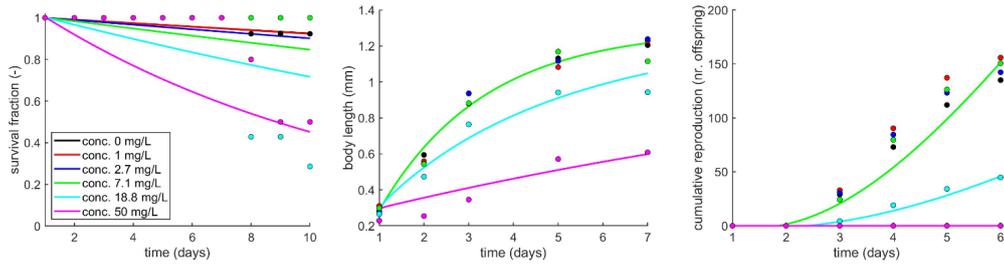
B) 50 nm fluorescent aminated (positive)
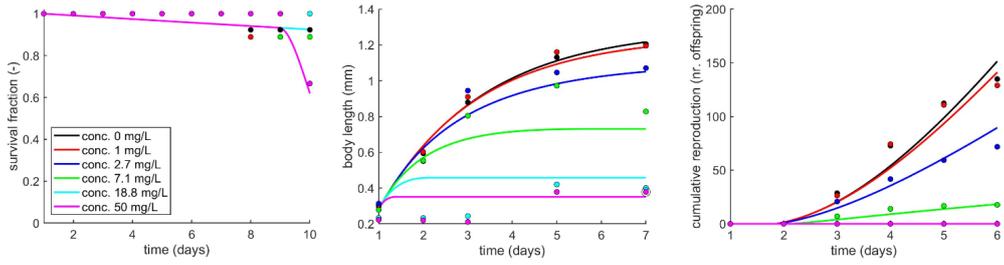
C) 50 nm fluorescent carboxylated (negative)
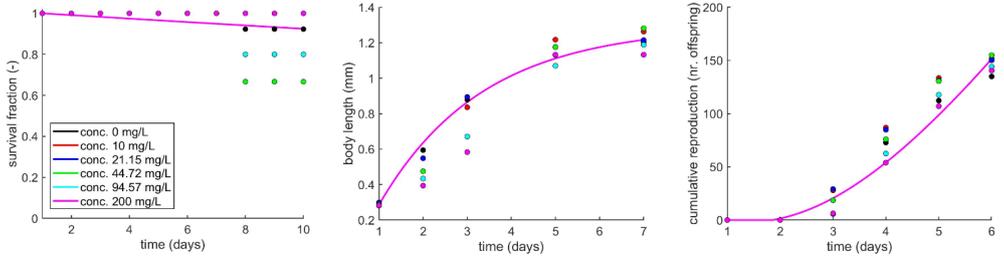
A) 60 nm polystyrene unfunctionalised (neutral)
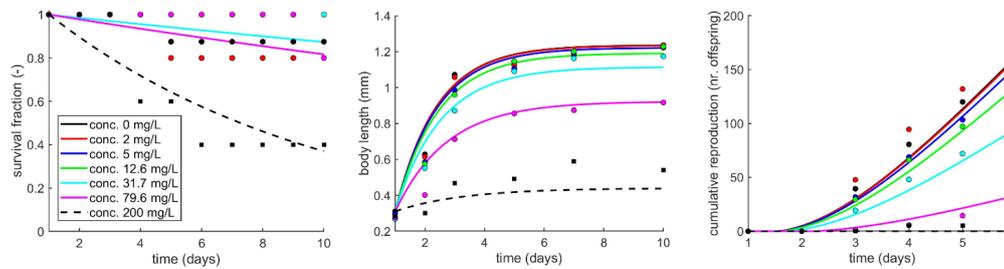
B) 60 nm aminated (positive)
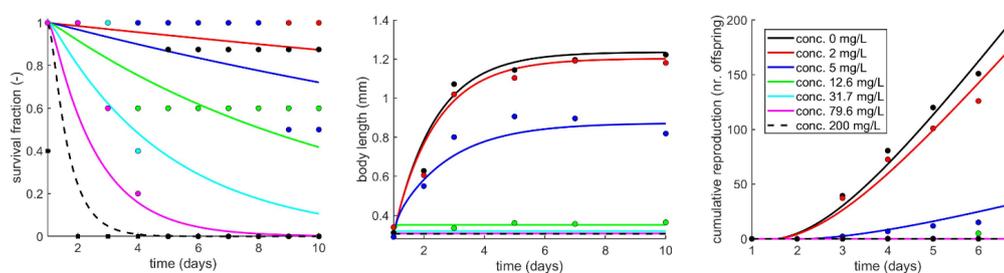
C) 60 nm carboxylated (negative)
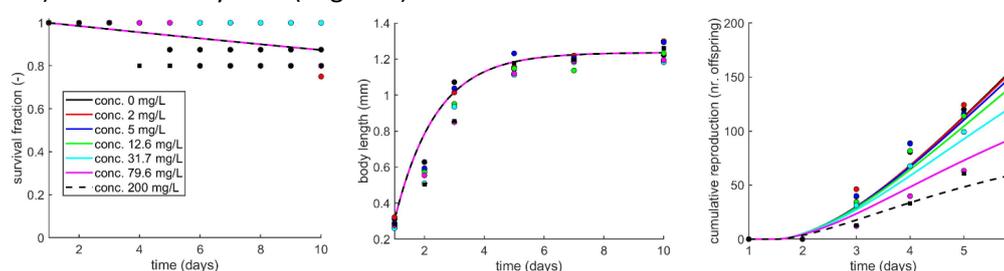
Figure 3. Observed (points) and simulated (lines) effect of A) 50-nm nanopolystyrene unfunctionalised particle (neutral), B) 50-nm aminated (+ve) nanopolystyrene particles, C) 50-nm carboxylated (-ve) nanopolystyrene particles, D) 60-nm polystyrene unfunctionalised (neutral) nanopolystyrene particles, E) 60-nm aminated (+ve) nanopolystyrene particles, and F) 60-nm carboxylated (-ve) nanopolystyrene particles on the life-cycle of *C. elegans* from DEBtox models fitted simultaneously for all nanoplastic types; for A) the best fit was with the physiological modes of action (pMoAs): growth and reproduction; for B), D) and E), the best fit was with the pMoAs: assimilation, growth and reproduction; for F) the best fit was with the pMoA: reproduction.

The life-cycle data was used for DEBtox modelling to estimate a series of TK and TD trait related parameters including the pMoA. Modelling of the underlying pMoAs showed that for the most toxic +ve nanoplastics in both sizes, the effects seen were in both cases best explained by a combined mechanism of reduced assimilation and increased costs for growth and reproduction (see Table S2 for goodness-of fit of the different pMoA models). For the two neutral particles, the $60PS^0$ particles had effects that were also best described by effects on assimilation and costs for growth and reproduction. For the $50PSF^0$ nanoplastics, the model did not support an effect on assimilation, but did for effects on costs for growth and reproduction, indicating that effects seen may not simply be related to the mechanisms of particle ingestion reducing food intake seen in previous work[52]. This suggests that while all the tested polystyrene nanoplastics all affected costs for growth and reproduction, the neutral smaller sized polystyrene nanoplastics had a more limited effect on feeding and the resulting assimilation of energy from food compared to the larger particles. For the two -ve nanoplastics, the low level of observed toxicity meant that DEBtox model could only be fitted for the $50CAF^-$ form. The best fitting pMoA for this particle was an effect only on costs for reproduction (Table S2).

The effects of nanoplastic exposure on assimilation of energy from food that were indicated for the $50AMF^+$, $60AM^+$ and $60AM^0$ variants[53,54] could be attributable to the presence of nanoplastics reducing the nutrition value of the diet, especially if they are ingested alongside

402 the larger bacteria , thus, diluting the food source (as observed in other species, e.g.[4], but not

403 to our knowledge in *C. elegans*). Food dilution would, however, affect all our treatments in the

404 same way and so would be unlikely to cause the different observed between the differently

405 changed particles. Alternative to food dilution, the effects indicated on assimilation could result

406 instead from direct effects on feeding rate[55], or instead through impacts on cellular energy

407 mechanisms through, for example, mitochondrial toxicity[26]. Micro- and nanoplastics exposures

408 have previously been linked to increased cellular oxidative stress, including in nematodes[13,14],

409 that has been linked to effects on metabolism (isocitrate dehydrogenase and lactate

410 dehydrogenase activity)[56] and depolarization of mitochondrial and cell membrane, chlorophyll

411 and population growth[10]. Further studies would be needed to address the basis of the effects.

412 Indeed, exposure effects on assimilation are not uniquely found for plastics, as this pMoA has

413 been widely attributed for a range of inorganic and organic chemicals. For example, the effects

414 of cadmium exposure on assimilation life-cycle tests have been found from DEBtox modelling

415 in both *C. elegans* and the collembolan *Folsomia candida*[26,57,58] and for uranium in *C. elegans*

416 [58] [59] indicating this as a common and conserved mechanism of effect.

417

418 Although the DEBtox modelling suggested common nanoplastic effect on assimilation and

419 costs for reproduction and growth, the DEBtox TK/TD parameters can be further used to

420 assess the detailed nature and strength of these toxicological effects (Table 2). Consistent

421 with our hypothesis, these differed between the tested nanoplastics. The dominant rate

422 constant 'k_d' governs the time needed for the damage density to reach steady state with the

423 external concentration, it is the mathematically equivalent to the elimination rate 'k_e' in the

424 previous DEBtox model structure[60]. The DEBtox model considers that individuals have a

425 threshold of the damage level for the budget energy 'z_b' and for survival 'z_s'. Once those values

426 are exceeded, the effects are proportional to the values of the damage above the thresholds

427 multiplied by an effect strength on energy-budget 'b_b' and on survival 'b_s'. This is the equivalent

428 of the no effect concentration (NEC) and the killing rate in previous DEBtox model. The effect

429 strength for energy-budget (b_b) and for survival (b_s) provides an indication of the damage

430 associated with the a given internal exposure for the energy budget and survival, respectively.

431

432 **Table 2.** Parameters values of the DEBtox model used for the models fitted for the charge

433 variant 50-nm fluorescent and 60-nm polystyrene nanoplastic sets

434

Parameter (symbol)	Description	Value 50-nm (95% CI)	Value 60-nm (95% CI)	Unit
Parameters fitted to the control treatment				
L_0	Body length at start experiment	0.29	0.31	mm
L_p	Body length at puberty	0.59	0.63	mm
L_m	Maximum body length	1.29	1.24	mm
r_B	Von Bertalanffy growth rate	0.43	0.72	1/d
R_m	Maximum reproduction rate	69.3	52.3	eggs/d
F	Scaled functional response	1	1	[-]
h_b	Background hazard rate	0.009	0.015	1/d
Toxicological parameters polystyrene aminated (+ve)				
k_d	Dominant rate constant	0.68 (0.59 - 1.17)	8.0 (7.2 - 8.4)	1/d
z_b	Threshold energy budget	0.59 (0.29 - 1.11)	1.7 (1.4 - 1.8)	mg/L
b_b	Effect strength energy-budget	0.07 (0.05 - 0.27)	0.09 (0.08 - 0.1)	L/mg
z_s	Threshold survival	49.8 (8.6 - 49.9)	2.31 (0 - 11)	mg/L
b_s	Effect strength survival	6.0 (0.2 - 189.1)	0.008 (0.004 - 0.014)	L/mg/d
Toxicological parameters for polystyrene unfunctionalised (neutral)				
k_d	Dominant rate constant	100* (4.35 – 100*)	100* (2.9 – 100*)	1/d
z_b	Threshold energy budget	14.0 (10.8 - 16.0)	1.4 (0 - 3.5)	mg/L
b_b	Effect strength energy-budget	0.16 (0.11 - 0.25)	0.003 (0.003 - 0.004)	L/mg
z_s	Threshold survival	2.7 (0 - 14.24)	69.4 (0 - 123)	mg/L
b_s	Effect strength survival	0.0017 (0.0006 - 0.0038)	0.0007 (0.0001 - 0.002)	L/mg/d
Toxicological parameters for polystyrene carboxylated (-ve)				
k_d	Dominant rate constant	Cannot be estimated	0.008 (0.001* - 100*)	1/d
z_b	Threshold energy budget	>200	0.025 (0 - 4.979)	mg/L
b_b	Effect strength energy-budget	Cannot be estimated	0.36 (0.05 – 100*)	L/mg
z_s	Threshold survival	>200	>200	mg/L
b_s	Effect strength survival	Cannot be estimated	Cannot be estimated	L/mg/d

435 * Boundary of the parameter space explorer

436

437 The few toxicological effects of the -ve nanoplastics make an analyses of the TK/TD parameter

438 values difficult due to the large confidence intervals estimated for the calculable values (Figure

439 3, Table 2). The DEBtox modelled values can, however, be compared between the +ve and

440 neutral nanoplastics (Table 2). The k_d values for the nanoplastics decreased from the neutral

441 to +ve particles. Thus, the neutral particle showed a k_d of 100 (for both size, Table 2), which

442 was the boundary for the algorithm, indicating an infinite value, suggesting a very fast uptake

443 leading immediately to damage, compared to a slower uptake leading to damage for the +ve

444 particles. Hence, the TK parameters point to a more rapid effect for the neutral nanoplastic,

445 which is not consistent with the hypothesis that +ve charge enhanced interactions between

446 the nanoplastics and membrane surfaces or of greater potency driven by greater uptake for

447 the +ve forms. For the TD parameters, the thresholds for effect on energy budget are smaller

448 for the +ve than for the neutral particles for the 50-nm materials. For $60PS^0$ the threshold for

449 energy budget (1.4) is close to those of $50AMF^+$ and $60AM^+$ (0.59 and 1.7 respectively), but

450 these particles show a smaller b_b value (0.003) than either charged particle (0.07 and 0.09

451 respectively). The values suggest that once the effect threshold is exceeded, the +ve particles

452 exert greater toxicity relative to their exposure concentration. DEBtox modelling, thus,

453 suggests a greater potential for damage associated with the +ve nanoplastics as the major

454 driver for their greater observed potency. Taken together the DEBtox pMoA model fits and

455 parameter values suggest that exposure to different surface functionalised nanoplastics has

456 an effect on life-cycle traits governed through effects on assimilation as well as direct toxicity

457 for growth and reproduction (potentially through germline effects according to[45]). The +ve

458 surface charge means that these effects to occur at lower internal thresholds and/or greater

459 toxicity for endpoint based for the same extent of accumulation. This greater impact may be

460 related to the potential of charge properties to cause greater disruption and damage,

461 potentially through their ability to interact with, and potentially traverse, cell members to reach

462 internal structures. Further studies with other different functionally charge particles are,

463 however, needed to confirm these patterns of charge related response.

464

465   Effects of organic matter eco-corona formation on relative toxicity of charged nanoplastics

466   The studies in the SPPW were conducted in a medium that did not contain any added

467   dissolved humic or fulvic acids. Forest and Pourchez[18] suggested the surface attachment of

468   proteins and other organic molecules can potentially modify the nature of nanomaterial

469   interactions with cell and organism surfaces. In natural soil and litter environments, exposure

470   to nanoplastics would normally take place in pore water in the presence of a complex mixture

471   of dissolved organic carbon species, such as humic and fulvic acid, carbohydrates, lipid

472   components, amino acids and larger biomolecules like DNA, peptides and proteins[61]. These

473   organic molecules may interact with particle surface to form an "eco-corona" that may change

474   surface properties to affect organism interactions[17,62]. While over the duration of the test

475   period, the presence of both the nematode itself and also the supplied bacterial food, will result

476   in an increase in the presence of small organic molecules in the test medium, the

477   concentrations and nature of dissolved organic molecules reached in the SSPW exposures

478   are unlikely to match those found in the soil solution environment in which meiofauna, such

479   as nematodes, would normal live.

480

481   To understand how exposure to a higher environmentally realistic concentration of dissolved

482   organic matter molecules may affect that nature of charge dependent toxicity of nanoplastics,

483   we repeated the toxicity testing for the 50-nm nanoplastic set in a LUFA2.2 soil pore water

484   extract. Exposures in pore water decreased the reproductive toxicity and growth inhibition

485   effects of all 50-nm particles compared to the SSPW tests (Figure 4 compared to Figure 2),

486   consistent with observations of other nanomaterials[63]. For the aminated materials, the only

487   functionalised for which a logistic model could be fitted in both media, toxicity was reduced 37

488   fold for the 50AMF$^+$ and 13 fold for the 60AM$^+$ nanoplastics in LUFA2.2 pore water compared

489   to SSPW (n.b. 50PSF^0, 50 CAF$^-$,reproduction EC$_{50}$ values >200 mg/L in all cases). Despite

490   the overall reduction in toxicity seen for both reproduction (Figure 4A) and growth (Figure 4B),

491   the 50AMF$^+$ retained increased potency to both measured endpoints in the LUFA2.2 pore

492   water compared to 50PSF[0] and 50CAF[-] nanoplastics despite the potential interactions of the

493   dissolved organic substance present with the particle surfaces.

494
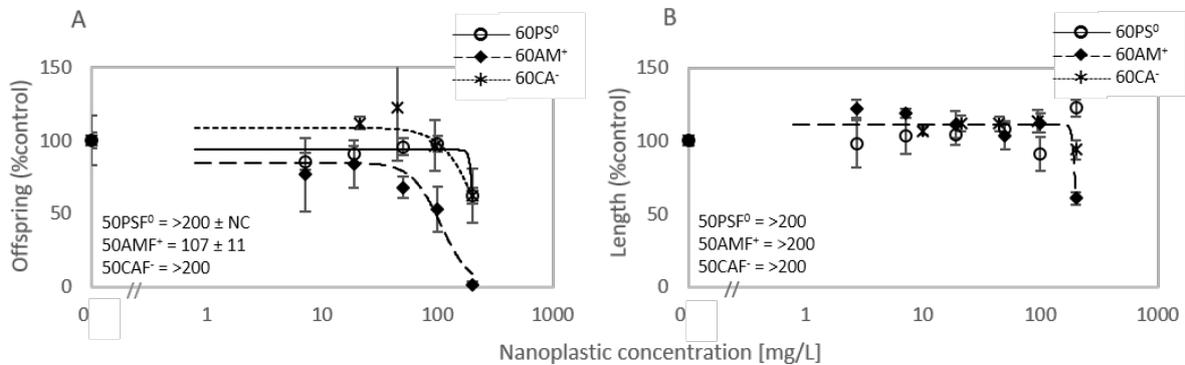
496   **Figure 4:** A. Number of offspring produced per individual after 6 days and B. volumetric length

497   at 72h expressed as % of control after exposure to 50PSF[0] (open circle, solid line), 50AMF[+]

498   (closed diamond, dashed line) and 50CAF[-] (asterisks, dotted line) in LUFA2.2 pore water

499   extract, point are averages ± SD from n=5 replicates, line is 3-parameter log logistic regression

500   fitted; stated values are EC_{50} (±SE) in mg/L , NC = confidence intervals not calculable.

501

502

503   Previous work has investigated the interaction of organic molecules with the surfaces of

504   differently charged nanomaterials. In a study conducted with bottle and tap drinking and

505   untreated lake waters, chemistry parameters including natural organic matter concentrations

506   were found to affect the surface properties and aggregation dynamics of polystyrene

507   nanoplastics. Different drivers of aggregation were identified, with cation adsorption likely to

508   promote aggregation for -ve and organic matter for +ve nanoplastics[64]. The SSPW used is

509   designed to mimic the soil pore water cation composition[49]. Hence, the major difference

510   between the two media is the presence of organic molecules in the extracted soil pore water.

511   Based on the effects of organic matter association being greater for the +ve nanoplastics[64],

512   the exposure in the LUFA2.2 porewater would be expected to lead to greater agglomeration

513   of the 50AMF[+] and 60AM[+] materials compared to the neutral and -ve forms. This may be

514   expected to lead to a greater reduction in +ve nanoplastic toxicity than that of the other forms.

515   However, the reduction found for the neutral nanoplastics also suggests that the association

516   of organic matter with the particle surface may also change interaction with nematodes that

517   reduces toxicity for these forms[65,66]. Hence, a wider mechanism of adsorbed organic molecule

518   passivation of nanoplastic effects independent of any charge providing surface

519   functionalisation is indicated. The presence of organic matter in soil pore water extract, thus,

520   mitigates the toxicity of each nanoplastic or changes palatability, greatly reducing effect on

521   life-cycle traits of all charged forms. Hence, although strong charge effects leading to toxicity

522   may occur in classical laboratory tests systems which often lack the presence of added

523   dissolved organic matter, these differences may not be fully realised in nature as natural ligand

524   pacify surface to reduce the strength of cellular interactions. Such results will be important for

525   understanding the hazard of different nanoplastics forms under realistic exposure conditions

526   providing insights for grouping and risk assessment.

527

535

536

537   REFERENCES

538   1.   Mitrano, D. M.; Beltzung, A.; Frehland, S.; Schmiedgruber, M.; Cingolani, A.; Schmidt,

539   F., Synthesis of metal-doped nanoplastics and their utility to investigate fate and behaviour in

540   complex environmental systems. *Nature Nanotech* **2019**, 362–368.

541   2.   Barbosa, F.; Adeyemi, J. A.; Bocato, M. Z.; Comas, A.; Campiglia, A., A critical

542   viewpoint on current issues, limitations, and future research needs on micro- and nanoplastic

543   studies: From the detection to the toxicological assessment. *Environmental Research* **2020,**

544   *182*, 109089.

545   3.   Enfrin, M.; Lee, J.; Gibert, Y.; Basheer, F.; Kong, L. X.; Dumee, L. F., Release of

546   hazardous nanoplastic contaminants due to microplastics fragmentation under shear stress

547   forces. *J. Hazardous Mat.* **2020,** *384*, 9.

548   4.   Horton, A. A.; Walton, A.; Spurgeon, D. J.; Lahive, E.; Svendsen, C., Microplastics in

549   freshwater and terrestrial environments: Evaluating the current understanding to identify the

550   knowledge gaps and future research priorities. *Sci. Total Environ.* **2017,** *586*, 127-141.

551   5.   Ng, E. L.; Lwanga, E. H.; Eldridge, S. M.; Johnston, P.; Hu, H. W.; Geissen, V.; Chen,

552   D. L., An overview of microplastic and nanoplastic pollution in agroecosystems. *Sci. Total*

553   *Environ.* **2018,** *627*, 1377-1388.

554   6.   Liu, Z.; Yu, P.; Cai, M.; Wu, D.; Zhang, M.; Huang, Y.; Zhao, Y., Polystyrene

555   nanoplastic exposure induces immobilization, reproduction, and stress defense in the

556   freshwater cladoceran *Daphnia pulex*. *Chemosphere* **2019,** *215*, 74-81.

557   7.   Lu, Y.; Zhang, Y.; Deng, Y.; Jiang, W.; Zhao, Y.; Geng, J.; Ding, L.; Ren, H., Uptake

558   and accumulation of polystyrene microplastics in zebrafish (*Danio rerio*) and toxic effects in

559   liver. *Environ. Sci. Technol.* **2016,** *50*, (7), 4054-4060.

560   8.   Jovanovic, B., Ingestion of microplastics by fish and its potential consequences from a

561   physical perspective. *Int. Environ. Assess. Man.* **2017,** *13*, (3), 510-515.

562   9.   Zhang, W. Y.; Liu, Z. Q.; Tang, S. K.; Li, D. M.; Jiang, Q. C.; Zhang, T. Q.,

563   Transcriptional response provides insights into the effect of chronic polystyrene nanoplastic

564   exposure on *Daphnia pulex*. *Chemosphere* **2020,** *238*, 9.

565   10.   Sendra, M.; Staffieri, E.; Yeste, M. P.; Moreno-Garrido, I.; Gatica, J. M.; Corsi, I.;

566   Blasco, J., Are the primary characteristics of polystyrene nanoplastics responsible for toxicity

567   and ad/absorption in the marine diatom *Phaeodactylum tricornutum*? *Environ. Pollut.* **2019,**

568   *249*, 610-619.

569 11.   Shao, H. M.; Han, Z. Y.; Krasteva, N.; Wang, D. Y., Identification of signaling cascade

570 in the insulin signaling pathway in response to nanopolystyrene particles. *Nanotoxicology*

571 **2019,** *13*, (2), 174-188.

572 12.   Yang, Y. H.; Wu, Q. L.; Wang, D. Y., Epigenetic response to nanopolystyrene in

573 germline of nematode *Caenorhabditis elegans*. *Ecotox. Environ. Saf.* **2020,** *206*, 9.

574 13.   Kim, H. M.; Long, N. P.; Min, J. E.; Anh, N. H.; Kim, S. J.; Yoon, S. J.; Kwon, S. W.,

575 Comprehensive phenotyping and multi-omic profiling in the toxicity assessment of

576 nanopolystyrene with different surface properties. *J. Hazardous Mat.* **2020,** *399*, 15.

577 14.   Yu, Y. J.; Chen, H. B.; Hua, X.; Dang, Y.; Han, Y. J.; Yu, Z. L.; Chen, X. C.; Ding, P.;

578 Li, H., Polystyrene microplastics (PS-MPs) toxicity induced oxidative stress and intestinal

579 injury in nematode *Caenorhabditis elegans*. *Sci. Total Environ.* **2020,** *726*.

580 15.   Silva, T.; Pokhrel, L. R.; Dubey, B.; Tolaymat, T. M.; Maier, K. J.; Liu, X. F., Particle

581 size, surface charge and concentration dependent ecotoxicity of three organo-coated silver

582 nanoparticles: Comparison between general linear model-predicted and observed toxicity. *Sci.*

583 *Total Environ.* **2014,** *468*, 968-976.

584 16.   El Badawy, A. M.; Silva, R. G.; Morris, B.; Scheckel, K. G.; Suidan, M. T.; Tolaymat, T.

585 M., Surface charge-dependent toxicity of silver nanoparticles. *Environ. Sci. Technol.* **2011,** *45*,

586 (1), 283-287.

587 17.   Spurgeon, D. J.; Lahive, E.; Schultz, C. L., Nanomaterial transformations in the

588 environment: Effects of changing exposure forms on bioaccumulation and toxicity. *Small* **2020**,

589 2000618.

590 18.   Forest, V.; Pourchez, J., Preferential binding of positive nanoparticles on cell

591 membranes is due to electrostatic interactions: A too simplistic explanation that does not take

592 into account the nanoparticle protein corona. *Materials Science and Engineering: C* **2017,** *70*,

593 889-896.

594 19.   Collin, B.; Tsyusko, O. V.; Starnes, D. L.; Unrine, J. M., Effect of natural organic matter

595 on dissolution and toxicity of sulfidized silver nanoparticles to *Caenorhabditis elegans*.

596 *Environ. Sci. Nano.* **2016,** *3*, (4), 728-736.

597   20.   Bozich, J. S.; Lohse, S. E.; Torelli, M. D.; Murphy, C. J.; Hamers, R. J.; Klaper, R. D.,

598   Surface chemistry, charge and ligand type impact the toxicity of gold nanoparticles to *Daphnia*

599   *magna*. *Environ. Sci. Nano.* **2014,** *1*, (3), 260-270.

600   21.   Saavedra, J.; Stoll, S.; Slaveykova, V. I., Influence of nanoplastic surface charge on

601   eco-corona formation, aggregation and toxicity to freshwater zooplankton. *Environ. Pollut.*

602   **2019,** *252*, 715-722.

603   22.   Libralato, G.; Galdiero, E.; Falanga, A.; Carotenuto, R.; de Alteriis, E.; Guida, M.,

604   Toxicity effects of functionalized quantum dots, gold and polystyrene nanoparticles on target

605   aquatic biological models: A review. *Molecules (Basel, Switzerland)* **2017,** *22*, (9), 1439.

606   23.   Sun, X. D.; Yuan, X. Z.; Jia, Y. B.; Feng, L. J.; Zhu, F. P.; Dong, S. S.; Liu, J. J.; Kong,

607   X. P.; Tian, H. Y.; Duan, J. L.; Ding, Z. J.; Wang, S. G.; Xing, B. S., Differentially charged

608   nanoplastics demonstrate distinct accumulation in *Arabidopsis thaliana*. *Nature Nanotech*

609   **2020**, 755–760.

610   24.   Della Torre, C.; Bergami, E.; Salvati, A.; Faleri, C.; Cirino, P.; Dawson, K. A.; Corsi, I.,

611   Accumulation and embryotoxicity of polystyrene nanoparticles at early stage of development

612   of sea urchin embryos *Paracentrotus lividus*. *Environ. Sci. Technol.* **2014,** *48*, (20), 12302-

613   12311.

614   25.   Wren, J. F.; Kille, P.; Spurgeon, D. J.; Swain, S.; Sturzenbaum, S. R.; Jager, T.,

615   Application of physiologically based modelling and transcriptomics to probe the systems

616   toxicology of aldicarb for *Caenorhabditis elegans* (Maupas 1900). *Ecotoxicology* **2011,** *20*, (2),

617   397-408.

618   26.   Swain, S.; Wren, J.; Stürzenbaum, S. R.; Kille, P.; Jager, T.; Jonker, M. J.; Hankard,

619   P. K.; Svendsen, C.; Chaseley, J.; Hedley, B. A.; Blaxter, M.; Spurgeon, D. J., Linking toxicants

620   mechanism of action and physiological mode of action in *Caenorhabditis elegans*. *BMC Sys.*

621   *Biol.* **2010,** *4*, 32.

622   27.   Ashauer, R.; Jager, T., Physiological modes of action across species and toxicants:

623   the key to predictive ecotoxicology. *Environ. Sci. Process. Impacts* **2018,** *20*, 48-57.

624 28. Nasser, F.; Constantinou, J.; Lynch, I., Nanomaterials in the environment acquire an

625 "eco-corona" impacting their toxicity to *Daphnia magna*-a call for updating toxicity testing

626 policies. *Proteomics* **2019,** *20*, e1800412.

627 29. Wagner, S.; Gondikas, A.; Neubauer, E.; Hofmann, T.; von der Kammer, F., Spot the

628 difference: engineered and natural nanoparticles in the environment--release, behavior, and

629 fate. *Angewandte Chemie* **2014,** *53*, (46), 12398-419.

630 30. Nasser, F.; Lynch, I., Secreted protein eco-corona mediates uptake and impacts of

631 polystyrene nanoparticles on *Daphnia magna*. *J. Proteom.* **2016,** *137*, 45-51.

632 31. Qie, Y. Q.; Yuan, H. F.; von Roemeling, C. A.; Chen, Y. X.; Liu, X. J.; Shih, K. D.;

633 Knight, J. A.; Tun, H. W.; Wharen, R. E.; Jiang, W.; Kim, B. Y. S., Surface modification of

634 nanoparticles enables selective evasion of phagocytic clearance by distinct macrophage

635 phenotypes. *Sci. Rep.* **2016,** *6*.

636 32. Kloet, S. K.; Walczak, A. P.; Louisse, J.; van den Berg, H. H. J.; Bouwmeester, H.;

637 Tromp, P.; Fokkink, R. G.; Rietjens, I., Translocation of positively and negatively charged

638 polystyrene nanoparticles in an in vitro placental model. *Toxicology in Vitro* **2015,** *29*, (7),

639 1701-1710.

640 33. Brenner, S., Genetics of *Caenorhabditis elegans*. *Genetics* **1974,** *77*, (1), 71-94.

641 34. Tyne, W.; Little, S.; Spurgeon, D. J.; Svendsen, C., Hormesis depends upon the life-

642 stage and duration of exposure: Examples for a pesticide and a nanomaterial. *Ecotox. Environ.*

643 *Saf.* **2015,** *120*, 117-123.

644 35. Hanna, S. K.; Bustos, A. R. M.; Peterson, A. W.; Reipa, V.; Scanlan, L. D.; Coskun, S.

645 H.; Cho, T. J.; Johnson, M. E.; Hackley, V. A.; Nelson, B. C.; Winchester, M. R.; Elliott, J. T.;

646 Petersen, E. J., Agglomeration of *Escherichia coli* with positively charged nanoparticles can

647 lead to artifacts in a standard *Caenorhabditis elegans* toxicity assay. *Environ. Sci. Technol.*

648 **2018,** *52*, (10), 5968-5978.

649 36. Stiernagle, T., Maintenance of *C. elegans.* In *C elegans A Practical Approach*, Hope,

650 I. A., Ed. Oxford University Press: Oxford, 1999; pp 51–57.

651   37.   Motulsky, H.; Christopoulos, A., *Fitting models to biological data using linear and*

652   *nonlinear regression: a practical guide to curve fitting*. Oxford University Press: 2004.

653   38.   Jager, T., Revisiting simplified DEBtox models for analysing ecotoxicity data. *Ecol.*

654   *Model.* **2020,** *416*, 108904.

655   39.   Jager, T.; Albert, C.; Preuss, T. G.; Ashauer, R., General Unified Threshold Model of

656   Survival - a toxicokinetic-toxicodynamic framework for ecotoxicology. *Environ. Sci. Technol.*

657   **2011,** *45*, (7), 2529-2540.

658   40.   Alda Alvarez, O. A.; Jager, T.; Kooijman, S. A. L. M.; Kammenga, J. E., Responses to

659   stress of *Caenorhabditis elegans* populations with different reproductive strategies. *Funct.*

660   *Ecol.* **2005,** *19*, (5), 656-664.

661   41.   Cedergreen, N.; Norhave, N. J.; Svendsen, C.; Spurgeon, D. J., Variable temperature

662   stress in the nematode *Caenorhabditis elegans* (Maupas) and its implications for sensitivity to

663   an additional chemical stressor. *PLOS One* **2016,** *11*, (1), e0140277.

664   42.   Pikuda, O.; Xu, E. G.; Berk, D.; Tufenkji, N., Toxicity assessments of micro- and

665   nanoplastics can be confounded by preservatives in commercial formulations. *Environmental*

666   *Science & Technology Letters* **2019,** *6*, (1), 21-25.

667   43.   Loos, C.; Syrovets, T.; Musyanovych, A.; Mailänder, V.; Landfester, K.; Nienhaus, G.

668   U.; Simmet, T., Functionalized polystyrene nanoparticles as a platform for studying bio–nano

669   interactions. *Beilstein Journal of Nanotechnology* **2014,** *5*, 2403-2412.

670   44.   Nolte, T. M.; Hartmann, N. B.; Kleijn, J. M.; Garnaes, J.; van de Meent, D.; Hendriks,

671   A. J.; Baun, A., The toxicity of plastic nanoparticles to green algae as influenced by surface

672   modification, medium hardness and cellular adsorption. *Aquat. Toxicol.* **2017,** *183*, 11-20.

673   45.   Qu, M.; Qiu, Y. X.; Kong, Y.; Wang, D. Y., Amino modification enhances reproductive

674   toxicity of nanopolystyrene on gonad development and reproductive capacity in nematode

675   *Caenorhabditis elegans*. *Environ. Pollut.* **2019,** *254*.

676   46.   Qu, M.; Wang, D. Y., Toxicity comparison between pristine and sulfonate modified

677   nanopolystyrene particles in affecting locomotion behavior, sensory perception, and neuronal

678   development in *Caenorhabditis elegans*. *Sci. Total Environ.* **2020,** *703*.

679 47. Marques-Santos, L. F.; Grassi, G.; Bergami, E.; Faleri, C.; Balbi, T.; Salis, A.;

680 Damonte, G.; Canesi, L.; Corsi, I., Cationic polystyrene nanoparticle and the sea urchin

681 immune system: biocorona formation, cell toxicity, and multixenobiotic resistance phenotype.

682 *Nanotoxicology* **2018,** *12*, (8), 847-867.

683 48. Pinsino, A.; Bergami, E.; Della Torre, C.; Vannuccini, M. L.; Addis, P.; Secci, M.;

684 Dawson, K. A.; Matranga, V.; Corsi, I., Amino-modified polystyrene nanoparticles affect

685 signalling pathways of the sea urchin (*Paracentrotus lividus*) embryos. *Nanotoxicology* **2017,**

686 *11*, (2), 201-209.

687 49. Tyne, W.; Lofts, S.; Spurgeon, D. J.; Jurkschat, K.; Svendsen, C., A new medium for

688 *Caenorhabditis elegans* toxicology and nanotoxicology studies designed to better reflect

689 natural soil solution conditions. *Environ. Toxicol. Chem.* **2013,** *32*, (8), 1711-1717.

690 50. Schultz, C.; Unrine, J.; Tsyusko, O.; Svendsen, C.; D.J., S., The transgenerational

691 toxicity of Ag ions, nanopaticles and sulphadised nanoparticles across 10 *Caenorhabditis*

692 *elegans* generations. *Proc. Royal Soc. B* **2016,** *283*, 20152911.

693 51. Polak, N.; Read, D. S.; Jurkschat, K.; Matzke, M.; Kelly, F. J.; Spurgeon, D. J.;

694 Sturzenbaum, S. R., Metalloproteins and phytochelatin synthase may confer protection

695 against zinc oxide nanoparticle induced toxicity in Caenorhabditis elegans. *Comp. Biochem.*

696 *Physiol. C* **2014,** *160*, 75-85.

697 52. Mueller, M. T.; Fueser, H.; Trac, L. N.; Mayer, P.; Traunspurger, W.; Hoss, S., Surface-

698 related toxicity of polystyrene beads to nematodes and the role of food availability. *Environ.*

699 *Sci. Technol.* **2020,** *54*, (3), 1790-1798.

700 53. Watts, A. J. R.; Lewis, C.; Goodhead, R. M.; Beckett, S. J.; Moger, J.; Tyler, C. R.;

701 Galloway, T. S., Uptake and retention of microplastics by the shore crab *Carcinus maenas*.

702 *Environ. Sci. Technol.* **2014,** *48*, (15), 8823-8830.

703 54. Woods, M. N.; Hong, T. J.; Baughman, D.; Andrews, G.; Fields, D. M.; Matrai, P. A.,

704 Accumulation and effects of microplastic fibers in American lobster larvae (*Homarus*

705 *americanus*). *Mar. Pollut. Bull.* **2020,** *157*, 111280.

706   55.   Liao, C. M.; Chiang, K. C.; Tsai, J. W., Bioenergetics-based matrix population modeling

707   enhances life-cycle toxicity assessment of tilapia *Oreochromis mossambicus* exposed to

708   arsenic. *Environmental Toxicology* **2006,** *21*, (2), 154-165.

709   56.   Prokić, M. D.; Radovanović, T. B.; Gavrić, J. P.; Faggio, C., Ecotoxicological effects of

710   microplastics: Examination of biomarkers, current state and future perspectives. *TrAC Trends*

711   *in Analytical Chemistry* **2019,** *111*, 37-46.

712   57.   Jager, T.; Crommentuijn, T.; VanGestel, C. A. M.; Kooijman, S. A. L. M., Simultaneous

713   modeling of multiple end points in life-cycle toxicity tests. *Environ. Sci. Technol.* **2004,** *38*, (10),

714   2894-2900.

715   58.   Margerit, A.; Gomez, E.; Gilbin, R., Dynamic energy-based modeling of uranium and

716   cadmium joint toxicity to *Caenorhabditis elegans*. *Chemosphere* **2016,** *146*, 405-412.

717   59.   Goussen, B.; Beaudouin, R.; Dutilleul, M.; Buisset-Goussen, A.; Bonzom, J. M.; Pery,

718   A. R. R., Energy-based modelling to assess effects of chemicals on *Caenorhabditis elegans*:

719   A case study on uranium. *Chemosphere* **2015,** *120*, 507-514.

720   60.   Jager, T.; Zimmer, E. I., Simplified Dynamic Energy Budget model for analysing

721   ecotoxicity data. *Ecol. Model.* **2012,** *225*, 74-81.

722   61.   Poirier, N.; Sohi, S. P.; Gaunt, J. L.; Mahieu, N.; Randall, E. W.; Powlson, D. S.;

723   Evershed, R. P., The chemical composition of measurable soil organic matter pools. *Organic*

724   *Geochemistry* **2005,** *36*, (8), 1174-1189.

725   62.   Svendsen, C.; Walker, L. A.; Matzke, M.; Lahive, E.; Harrison, S.; Crossley, A.; Park,

726   B.; Lofts, S.; Lynch, I.; Vazquez-Campos, S.; Kaegi, R.; Gogos, A.; Asbach, C.; Cornelis, G.;

727   von der Kammer, F.; van den Brink, N. W.; Mays, C.; Spurgeon, D. J., Key principles and

728   operational practices for improved nanotechnology environmental exposure assessment.

729   *Nature Nanotech* **2020,** *15*, (9), 731-742.

730   63.   Hoss, S.; Fritzsche, A.; Meyer, C.; Bosch, J.; Meckenstock, R. U.; Totsche, K. U., Size-

731   and composition-dependent toxicity of synthetic and soil-derived Fe oxide colloids for the

732   nematode *caenorhabditis elegans*. *Environ. Sci. Technol.* **2015,** *49*, (1), 544-552.

733 64. Ramirez, L.; Gentile, S. R.; Zimmermann, S.; Stoll, S., Behavior of TiO2 and CeO2

734 nanoparticles and polystyrene nanoplastics in bottled mineral, drinking and lake geneva

735 waters. Impact of water hardness and natural organic matter on nanoparticle surface

736 properties and aggregation. *Water* **2019,** *11*, (4), 721.

737 65. Collin, B.; Oostveen, E.; Tsyusko, O. V.; Unrine, J. M., Influence of natural organic

738 matter and surface charge on the toxicity and bioaccumulation of functionalized ceria

739 nanoparticles in *Caenorhabditis elegans*. *Environ. Sci. Technol.* **2014,** *48*, (2), 1280-1289.

740 66. Wu, J.; Jiang, R.; Lin, W.; Ouyang, G. F., Effect of salinity and humic acid on the

741 aggregation and toxicity of polystyrene nanoplastics with different functional groups and

742 charges. *Environ. Pollut.* **2019,** *245*, 836-843.

743

744 SUPPORTING INFORMATION

745 EC_{50} values for 50 nm and 60 nm polystyrene nanoplastics for reproduction, volumetric length

746 and lifespan in SSPW; DEBtox model fit statistics; life-cycle data for the effects of the 50 nm

747 and 60 nm nanopolystyrene sets and images of exposure media at approximate EC_{50}

748 concentrations for reproduction illustrating absence of bacterial aggregates.